Weak Quasi-elastic Production of Hyperons

S. K. Singh[a,b] and M. J. Vicente Vacas[a]

[a] *Departamento de Física Teórica and IFIC,*

Centro Mixto Universidad de Valencia CSIC; Institutos de Investigación de Paterna,

Aptdo. 22085, 46071 Valencia, Spain.

[b] *Department of Physics, Aligarh Muslim University, Aligarh- 202002, India.**

(Dated: January 9, 2014)

Abstract

The quasielastic weak production of Λ and Σ hyperons from nucleons and nuclei induced by antineutrinos is studied in the energy region of some ongoing neutrino oscillation experiments in the intermediate energy region. The hyperon nucleon transition form factors determined from neutrino nucleon scattering and an analysis of high precision data on semileptonic decays of neutron and hyperons using SU(3) symmetry have been used. The nuclear effects due to Fermi motion and final state interaction effects due to hyperon nucleon scattering have also been studied. The numerical results for differential and total cross sections have been presented.

*Electronic address: pht13sks@rediffmail.com

I. INTRODUCTION

The study of weak nuclear reactions induced by neutrinos and antineutrinos in the energy region of few GeV has become quite important due to the role played by these processes in the analysis of various neutrino oscillation experiments being done with atmospheric and accelerator neutrinos in the intermediate energy region [1, 2, 3, 4]. In this energy region, the theoretical cross sections for various weak processes induced by neutrinos and antineutrinos on nucleons and nuclei are needed to model neutrino-nuclear interactions in Monte Carlo neutrino generators like NUANCE [5], NEUGEN [6], NEUT [7] or more general codes like FLUKA [8] which are being used by groups doing neutrino oscillation experiments. The dominant weak process of current interest is the quasi-elastic production of leptons induced by $\Delta S = 0$ charged and neutral weak currents which has been extensively studied in literature including nuclear effects using various approaches [9, 10, 11, 12, 13, 14, 15, 16, 17, 18, 19, 20, 21, 22]. However, in this energy region other processes in which pions, kaons and hyperons are produced can also be important. In particular, the inelastic processes where single pions are produced by weak charged and neutral currents have recently attracted much attention as they play a very important role in performing the background studies in the analysis of neutrino oscillation experiments. Many authors [23, 24, 25, 26, 27, 28, 29, 30] have recently studied the weak pion production from nucleons and nuclei in the energy region relevant for the ongoing neutrino oscillation experiments by K2K[2] and MiniBooNE collaborations[3]. In some of these studies the nuclear effects in the weak pion production process as well as in the final state interaction (FSI) of outgoing pions with the final nucleus have also been taken into account [25, 26, 27, 28, 29, 30].

There exist very few calculations for the neutrino production of strange baryons and mesons from free nucleons. In these calculations the hyperon nucleon transition form factors are determined either from the Cabibbo theory with SU(3) symmetry [31, 32] or from some quark models used for describing the baryon structure[33]. There are no calculations to our knowledge where nuclear effects have been included in the weak production of strange particles from nuclei induced by neutrinos. The neutrino production of strange particles is induced by weak charged as well as neutral currents. The weak neutral currents induce only $\Delta S = 0$ processes due to absence of Flavour Changing Neutral Currents (in the standard model). On the other hand, the weak charged currents induce both $\Delta S = 0$ and $\Delta S = 1$

processes. The production of strange particles through $\Delta S = 1$ processes is suppressed by a factor $tan^2\theta_c$ where θ_c is the Cabibbo angle, as compared to the $\Delta S = 0$ processes. However, in the low energy region of $E_\nu \sim 1 - 3$GeV, the associated production of strange particles through $\Delta S = 0$ processes is suppressed by phase space. Therefore, it is likely that in this low energy region, the cross sections for the production of strange particles through $\Delta S = 1$ and $\Delta S = 0$ processes become comparable. In the case of the weak production of strange particles through $\Delta S = 1$ processes, the $\Delta S = \Delta Q$ selection rule restricts the quasi elastic hyperon production to antineutrinos rather than neutrinos. As a consequence, in the $\Delta S = 1$ sector only antineutrino induced reactions like $\bar{\nu}_l + N \rightarrow l^+ + Y(Y^\star)$ where $Y(Y^\star)$ is a $S = -1$ hyperon (hyperon resonance) are allowed. Therefore, the only possible quasi-elastic $\Delta S = 1$ hyperon (Y) production processes allowed in the neutrino(antineutrino) induced reactions are

$$\bar{\nu}_l + p \ \rightarrow l^+ + \Lambda \tag{1}$$

$$\bar{\nu}_l + p \ \rightarrow l^+ + \Sigma^0 \tag{2}$$

$$\bar{\nu}_l + n \ \rightarrow l^+ + \Sigma^- \tag{3}$$

These reactions have been experimentally studied in past but the experimental information is very scanty and comes mainly from some older experiments performed with the Gargamelle [34, 35] and the SKAT [36] bubble chambers filled with heavy liquid like Freon and/or Propane [37]. The number of observed events was small leading to cross sections with large error bars due to poor statistics. However, the results for the cross sections were found to be consistent with predictions of the Cabibbo theory with SU(3) symmetry. A suppression of cross sections due to nuclear medium effects is clearly seen, specially in the experiments of Erriquez et al. [35] but no attempts have been made to theoretically estimate the nuclear medium effects on the weak production of hyperons from nuclei. An understanding of these nuclear effects would be useful for the analysis of future experiments which are being planned to study the weak production of strange particles in the context of neutrino oscillation and proton decay search experiments. Such experiments are planned with the NUMI beamline in the MINERVA experiment [38]. These reactions may also be seen at K2K and MiniBooNE where the effective reach of neutrino energy for cross section measurement could reach about 3 GeV [2, 3]. The study of weak production of strange particles is an important subject in itself as it helps to experimentally determine the momentum dependence of various transition

form factors and test the theoretical models proposed for SU(3) breaking in semileptonic $\Delta S = 1$ processes.

In this paper we report on the study of antineutrino induced quasi-elastic production of Λ and Σ hyperons from nucleons i.e. reactions (1) to (3) and also the effects of nuclear medium and final state interactions when these reactions take place on nucleons bound in nuclei. In section II, we describe the general formalism for calculating the differential and total cross section for the process $\bar{\nu}_l + N \rightarrow l^+ + Y$ using Cabibbo theory with SU(3) symmetry where the transition form factors for $N \rightarrow Y$ transitions are determined from a theoretical analysis of the latest experiments on semileptonic decay of hyperons, i.e $Y \rightarrow N + l^- + \bar{\nu}_l$. In section III, we describe the nuclear medium effects when these reactions take place in nuclei like ^{16}O or ^{56}Fe which are target nuclei for future detectors planned to be used in neutrino oscillation and proton decay search experiments. In section IV, we present the numerical results for total and differential cross sections for production of leptons and hadrons from nucleon and nuclear targets. We also consider the pion production due to the weak decay of the hyperons. Finally we summarize and give main conclusions of our work in the last section.

II. FORMALISM

A. Cross section and Matrix elements

The differential cross section $d\sigma$ for the process $\bar{\nu}_l(k) + N(p) \rightarrow l^+(k') + Y(p')$, with $q = p' - p = k - k'$ is given by

$$d\sigma = \frac{1}{(2\pi)^2} \frac{1}{4E_\nu \sqrt{s}} \delta^4(k + p - k' - p') \frac{d^3k'}{2E_{k'}} \frac{d^3p'}{2E_{p'}} |\mathcal{M}|^2 \tag{4}$$

leading to

$$\frac{d\sigma}{dQ^2} = \frac{1}{64\pi s E_\nu^2} |\mathcal{M}|^2 \tag{5}$$

where $s = (q + p)^2$, $E_\nu = \frac{s - M^2}{2\sqrt{s}}$ is the CM neutrino energy, M is the nucleon mass and $\mathcal{M}$ is the scattering amplitude matrix element written as

$$\mathcal{M} = \frac{G}{\sqrt{2}} a_c \bar{v}(k') \gamma^\mu (1 + \gamma^5) v(k) < Y(p') | V_\mu - A_\mu | N(p) >, \tag{6}$$

where $a_c = sin\theta_c$ for $\Delta S = 1$ processes and $a_c = cos\theta_c$ for $\Delta S = 0$ processes. The matrix elements $< Y(p')|V_\mu|N(p) >$ and $< Y(p')|A_\mu|N(p) >$ correspond to the transition matrix elements of the vector and axial currents V_μ and A_μ which are defined as

$$< Y(p')|V_\mu|N(p) >= \bar{u}_Y(p') \left[\gamma_\mu f_1(q^2) + i\sigma_{\mu\nu}\frac{q^\nu}{M+M_Y} f_2(q^2) + \frac{f_3(q^2)}{M_Y} q_\mu\right] u_N(p) \quad (7)$$

$$< Y(p')|A_\mu|N(p) >= \bar{u}_Y(p') \left[\gamma_\mu g_1(q^2) + i\sigma_{\mu\nu}\frac{q^\nu}{M+M_Y} g_2(q^2) + \frac{g_3(q^2)}{M_Y} q_\mu\right] \gamma^5 u_N(p) \quad (8)$$

where $f_i(q^2)$, and $g_i(q^2)$, $(i = 1, 2, 3)$ are the vector and axial vector transition form factors. In defining these matrix elements, we follow the Bjorken Drell [39] conventions for the Dirac matrices. The determination of these form factors is done using Cabibbo theory with SU(3) symmetry which describes the recent precision data on semileptonic decays of hyperons [40, 41] quite well. The corrections due to SU(3) breaking effects on semileptonic decays have been discussed in literature and are found to be small [42].

In the following, we briefly outline the procedure for determination of various vector and axial vector transition form factors $f_i(q^2)$ and $g_i(q^2)$ defined in equations 7 and 8.

B. Form Factors

In the standard model, the vector and axial vector currents V_μ and A_μ are defined as

$$V_\mu^i = \bar{q}\frac{\lambda^i}{2}\gamma_\mu q \quad (9)$$

$$A_\mu^i = \bar{q}\frac{\lambda^i}{2}\gamma_\mu\gamma_5 q \quad (10)$$

where $\frac{\lambda^i}{2}$ are the generators of flavour SU(3). Assuming that, V_μ^i and A_μ^i belong to the octet representation of flavour SU(3), and neglecting any SU(3) breaking effects, vector and axial vector transition form factors for all the N$\rightarrow$ Y transitions can be expressed in terms of two functions for vector(axial vector) current which could be determined from the experimental data on semileptonic decays of nucleons and hyperons. This is because, the coupling of initial and final baryon states belonging to an octet representation of SU(3), through an octet of vector (axial vector) currents is described in terms of two reduced matrix elements F and D corresponding to the antisymmetric and symmetric coupling of two octets of baryons in the initial and final state to the octet of vector (axial vector) currents, through SU(3) Clebsch Gordan coefficients. More precisely, the vector and axial vector form factors $f_i(q^2)$ and

$g_i(q^2)$ defined above are given in terms of the functions $F_i^V(q^2)$ and $D_i^V(q^2)$ corresponding to vector couplings and $F_i^A(q^2)$ and $D_i^A(q^2)$ corresponding to axial vector couplings as

$$f_i(q^2) = aF_i^V(q^2) + bD_i^V(q^2), (\text{i=1,2,3}) \tag{11}$$

$$g_i(q^2) = aF_i^A(q^2) + bD_i^A(q^2), (\text{i=1,2,3}) \tag{12}$$

The constants a and b are the SU(3) Clebsch Gordan coefficients given in Table I for the reactions of our present interest. We see that all the form factors for $p \to \Sigma^0$ are $\frac{1}{\sqrt{2}}$ times the form factors $n \to \Sigma^-$ transitions, leading to the prediction that $\frac{d\sigma}{dq^2}(\bar{\nu} + n \to \mu^+ + \Sigma^-)/\frac{d\sigma}{dq^2}(\bar{\nu} + p \to \mu^+ + \Sigma^0) = \frac{1}{2}$. This is reflection of the ΔI=$\frac{1}{2}$ rule, inherent in the Cabibbo theory of $\Delta S = 1$ weak processes.

Transitions	a	b
$p \to n$	1	1
$p \to \Lambda$	$-\sqrt{\frac{3}{2}}$	$-\sqrt{\frac{1}{6}}$
$n \to \Sigma^-$	-1	1
$p \to \Sigma^0$	$-\frac{1}{\sqrt{2}}$	$\frac{1}{\sqrt{2}}$

TABLE I: Values of the Form Factors coefficients a, b of Eqs. 11-12.

Furthermore, the assumption that V_μ and A_μ belong to the octet representation of flavour SU(3), implies that the symmetry properties of the ΔS=0 currents which are well verified in the study of $n \to p + e^- + \bar{\nu_e}$ decays are also obeyed by the the $\Delta S = \pm 1$ currents. Accordingly, we assume

(a) G invariance and SU(3) symmetry leading to prediction that $f_3(q^2) = g_2(q^2) = 0$.

(b) Conserved Vector Current and SU(3) symmetry leading to $f_3(q^2) = 0$ and determination of other vector transition form factors in terms of the electromagnetic form factors of protons and neutrons. The electromagnetic form factors of protons and neutrons in terms of nucleons ($N = p, n$) are defined through the matrix element of the electromagnetic current V_μ taken between the nucleon states ($N = p, n$) as $< N(p')|V_\mu^{em}|N(p) >$ and is written as

$$< N(p')|V_\mu^{em}|N(p) >= \bar{u}(p') \left[\gamma_\mu f_1^{N=p,n}(q^2) + i\sigma_{\mu\nu}\frac{q^\nu}{2M} f_2^{N=p,n}(q^2)\right] u(p) \tag{13}$$

where $f_1^{N=p,n}(q^2)$ are the electromagnetic form factors for nucleons. V_μ^{em} is the electromag-

netic current given by

$$V_\mu^{em} = V_\mu^3 + \frac{1}{\sqrt{3}} V_\mu^8 \tag{14}$$

where the superscripts 3 and 8 show SU(3) indices. Evaluating Eqn. 13 between the nucleon states using their SU(3) indices we get

$$\begin{aligned} f_i^n(q^2) &= -\frac{2}{3} D_i^V(q^2), \quad \text{i=1,2} \\ f_i^p(q^2) &= F_i^V(q^2) + \frac{1}{3} D_i^V(q^2), \quad \text{i=1,2} \end{aligned} \tag{15}$$

Eqns. 15, determine $F_i^V(q^2)$ and $D_i^V(q^2)$ in terms of the electromagnetic form factors for neutrons and protons $f_i^n(q^2)$ and $f_i^p(q^2)$ as

$$\begin{aligned} F_i^V(q^2) &= f_i^p(q^2) + \frac{1}{2} f_i^n(q^2) \\ D_i^V(q^2) &= -\frac{3}{2} f_i^n(q^2) \end{aligned} \tag{16}$$

Once $F_i^V(q^2)$ and $D_i^V(q^2)$ are determined, the transition vector form factors $f_1(q^2)$ and $f_2(q^2)$ defined in Eqn. 7 are determined for all transitions, in terms of $f_i^{p,n}(q^2)$ and are presented in table II. For $f_i^{p,n}(q^2)$ we take [43, 44]:

$$\begin{aligned} f_1^{p,n}(q^2) &= \frac{1}{(1-\frac{q^2}{4M^2})} \left[G_E^{p,n}(q^2) - \frac{q^2}{4M^2} G_M^{p,n}(q^2) \right] \\ f_2^{p,n}(q^2) &= \frac{1}{(1-\frac{q^2}{4M^2})} [G_M^{p,n}(q^2) - G_E^{p,n}(q^2)] \end{aligned}$$

where

$$G_E^p(q^2) = \left(1 - \frac{q^2}{M_V^2}\right)^{-2} \tag{17}$$

$$G_M^p(q^2) = (1+\mu_p) G_E^p(q^2), \; G_M^n(q^2) = \mu_n G_E^p(q^2);$$

$$G_E^n(q^2) = (\frac{q^2}{4M^2}) \mu_n G_E^p(q^2) \xi_n; \; \xi_n = \frac{1}{1 - \lambda_n \frac{q^2}{4M^2}}$$

$$\mu_p = 1.792847, \mu_n = -1.913043, M_V = 0.84 GeV, \text{ and } \lambda_n = 5.6.$$

The numerical value of the vector dipole mass M_V= 0.84 GeV is taken from experimental data on electron proton scattering. However, in the $\Delta S = 1$ sector with SU(3) symmetry a scaled value of M_V= 0.97 GeV has also been used in the analysis of semileptonic decays [40].

(c) The Partial Conservation of Axial Current (PCAC) hypothesis and SU(3) symmetry leads to the determination of the pseudo vector transition form factor $g_3(q^2)$ in terms of the axial vector form factor $g_1(q^2)$ which predicts $g_3(q^2) = \frac{2M^2}{m_\pi^2 - q^2} g_1(q^2)$. These form factors are determined from the experimental data on ΔS=0 neutrino scattering on nucleon and semileptonic hyperon decays. In these processes, the contribution of $g_3(q^2)$, being proportional to $\frac{m_l}{M}$, is small and is generally neglected in the analysis of neutrino scattering and semileptonic decays. Therefore, the q^2 dependence of $g_3(q^2)$ specially at higher q^2 is not determined experimentally. Some experimental information on $g_3(q^2)$ is available from studies on muon capture in nucleon and nuclei, which is consistent with the predictions of PCAC . However, the numerical contribution of $g_3(q^2)$ to the cross sections in the present reactions is also small and is neglected. With these assumptions the only undetermined form factor needed for the calculation of the matrix element defined in equations 7 and 8 is $g_1(q^2)$.

In order to determine q^2 dependence of transition form factors $g_1(q^2)$ for all transitions under present consideration one needs the q^2 dependence of $F_1^A(q^2)$ and $D_1^A(q^2)$ separately which is not available due to lack of high q^2 data from semileptonic processes in the$\Delta S = 1$ sector. We therefore, assume that $F_1^A(q^2)$ and $D_1^A(q^2)$ have the same q^2 dependence. From table I the axial vector form factor $g_1(q^2)$ is given by $g_1(q^2) = F_1^A(q^2) + D_1^A(q^2)$ for the $\nu_\mu + n \to \mu^- + p$ reaction. The determination of q^2 dependence of the axial vector form factor in $\nu_\mu + n \to \mu^- + p$ reaction yields information about the q^2 dependence of $F_1^A(q^2) + D_1^A(q^2)$.

We now assume that $F_1^A(q^2)$ and $D_1^A(q^2)$ separately have the q^2 dependence which is given by the the q^2 dependence of $g_A^{n\to p}(q^2)$, i.e. $g_1^{n\to p}(q^2) = g_1^{n\to p}(0)\left(1 - \frac{q^2}{M_A^2}\right)^{-2}$. We thus take

$$F_1^A(q^2) = F\left(1 - \frac{q^2}{M_A^2}\right)^{-2}, \quad \text{with } F = F_1^A(0)$$

and

$$D_1^A(q^2) = D\left(1 - \frac{q^2}{M_A^2}\right)^{-2}, \text{ with } \quad D = D_1^A(0).$$

The numerical value of the axial vector dipole mass M_A is taken from the analysis of world data on quasielastic neutrino nucleon scattering to be 1.03 GeV [44, 45]. However, the recent high statistics K2K experiment on quasielastic scattering at low energies suggests a higher value of $M_A = 1.20 \pm 0.12$ GeV [46]. On the other hand, the analysis of very low q^2 data on semileptonic decays of hyperons uses an axial dipole mass of M_A=1.25 GeV in ΔS=1 sector [40].

With this parametrization of $F_1^A(q^2)$ and $D_1^A(q^2)$, the constants F and D are determined from the analysis of present experimental data on semileptonic decays of nucleons and hyperons corresponding to very low q^2 which gives $F + D = 1.2670 \pm 0.0030$ and $F - D = -0.341 \pm 0.016$ [41]. Using these values of $F_1^A(q^2)$ and $D_1^A(q^2)$, we present in table II, the values of $g_1(q^2)$ for various transitions of our present interest in terms of $x = \frac{F_1^A(q^2)}{F_1^A(q^2)+D_1^A(q^2)} = \frac{F}{F+D}$ and $g_A(q^2) = (F+D)\left(1 - \frac{q^2}{M_A^2}\right)^{-2}$.

Transitions	$f_1(q^2)$	$f_2(q^2)$	$g_1(q^2)$
$n \to p$	$f_1^p(q^2) - f_1^n(q^2)$	$f_2^p(q^2) - f_2^n(q^2)$	$g_A(q^2)$
$p \to \Lambda$	$-\sqrt{\frac{3}{2}} f_1^p(q^2)$	$-\sqrt{\frac{3}{2}} f_2^p(q^2)$	$-\sqrt{\frac{3}{2}} \frac{(1+2x)}{3} g_A(q^2)$
$n \to \Sigma^-$	-$(f_1^p(q^2) + 2f_1^n(q^2))$	-$(f_2^p(q^2) + 2f_2^n(q^2))$	$(1-2x) g_A(q^2)$

TABLE II: Form Factors of Eqs. 7-8.

III. NUCLEAR MEDIUM AND FINAL STATE INTERACTIONS

A. Nuclear Effects

When the reactions shown in equations (1-3) take place on nucleons which are bound in the nucleus, certain constraints on their dynamics arising due to the Fermi motion and Pauli blocking effects of initial nucleons have to be considered. In the final state the produced hyperons are not subjected to any Pauli Blocking but are affected by the final state interactions with the nucleus through the hyperon nucleon quasi-elastic and charge exchange scattering processes. Moreover, the charged lepton in the final state moves in the Coulomb field of the final nucleus. However, in the energy region of 1- 3 GeV, the effect of Coulomb distortion of the charged lepton wave function is small and is neglected in the present calculations. The Fermi motion effects are calculated in a local Fermi Gas model where the the differential cross section for the process $\bar{\nu}_l + N \to l^+ + Y$ is now written as

$$d\sigma = \frac{1}{(2\pi)^2} 2 \int d^3\vec{r} \frac{d^3\vec{p}}{(2\pi)^3} n(p,r) \delta^4(k + p - k' - p') \frac{d^3\vec{k}'}{2E_{k'}} \frac{d^3\vec{p}'}{2E_{p'}} \frac{1}{4E_\nu^{CM}\sqrt{s}} |\mathcal{M}|^2 \qquad (18)$$

where $n(p,r)$ is the local occupation number of the initial nucleon of momentum p localized at a radius r in the nucleus, and is determined in the local density approximation. Here, E_ν^{CM} and s are the neutrino energy in the nucleon-neutrino CM system and the nucleon neutrino

invariant mass squared respectively. Solving the δ function of momentum conservation , we do the integration over the hyperon momentum $\vec{p}\,'$, and we use the δ function of energies to integrate the cosinus of the angle of the initial nucleon momentum $\vec{p}$. Then, the differential cross section for the quasielastic hyperon production from nuclei can be written as

$$d\sigma = \frac{1}{64\pi^4} \int r^2 dr d\phi_p \int_0^{k_F(r)} dp\; d^3\vec{k}\,' \frac{p}{E_\nu^{CM}\sqrt{s}E_\mu|\vec{k}-\vec{k}\,'|}|\mathcal{M}|^2 \tag{19}$$

with $k_F(r) = (\frac{3}{2}\pi^2\rho(r))^{\frac{1}{3}}$, where $\rho(r)$ is the target nucleon density in the nucleus which is taken from ref. [47] for the protons, and scaled with a factor N/Z for the neutrons. All kinematic variables are defined by the integral itself, except the cosinus of relative angle between $\vec{p}$ and $\vec{k}-\vec{k}\,'$ which is obtained from the δ function of energies.

To obtain these formulas we have followed a quasi-free approach where both Σ and Λ have been treated as stable particles, with a well defined energy for a given momentum. This is acceptable because both are quite narrow even in the nuclear medium, see i.e. ref. [48], where additional decay channels are present. Also, in the actual implementation of Eq. 19 when solving the δ of energies, we have neglected the real part of the hyperon optical potential in the nucleus. We have checked numerically that potentials of a typical size ($\approx -30MeV\rho/\rho_0$) do not modify appreciably the results.

B. Final State Interactions

The hyperons Λ^0, Σ^0, Σ^- which are produced in reactions (1-3) undergo elastic and charge exchange scattering with the nucleons present in the nucleus through strong interactions while some of the Σ^0 disappear through the electromagnetic decay channel $\Sigma^0 \to \Lambda^0 + \gamma$. Therefore the production cross sections for the hyperons from the nuclear targets are affected by the presence of the electromagnetic and strong interactions of final state hyperons in the nuclear medium. One of the interesting features of the final state interactions(FSI) of hyperons in the nuclear medium is the appearance of Σ^+ hyperons which are not produced in the basic weak process induced by the $\bar{\nu}$. This is due to charge exchange scattering processes like $\Lambda^0 + p \to \Sigma^+ + n$ and $\Sigma^0 + p \to \Sigma^+ + n$ which can take place in nuclei. The effect of FSI on the weak production cross section for Σ^0, Σ^- and Λ^0 and the appearance of Σ^+ are estimated with the help of a Monte Carlo code for propagation of hyperons in the nuclear medium using as input the scarce available experimental cross sections for the

hyperon nucleon scattering cross sections. We have compiled the parametrizations used in this work in the Appendix.

C. Monte Carlo simulation

¿From Eq. 18 we can obtain $\frac{d^6\sigma}{d^3r\,d^3k'}$ after performing the integration over the rest of variables. This profile function is then used as input for our Monte Carlo simulation. We generate hyperon production events by selecting a random position r and a momentum k' and assigning to the event the weight given by the profile function. We then assume the real part of the hyperons nuclear potential to be weak compared with their kinetic energies and propagate them following straight lines till they are out of the nucleus. To take into account the collisions we follow the hyperon by moving it a short distance dl, along its momentum direction, such that $P\,dl << 1$, where P is the probability of interaction per unit length. A random number $x \in [0, 1]$ is generated and we consider that an interaction has taken place when $P\,dl > x$. If no interaction occurs we repeat the procedure by moving the hyperon a new step dl.

The probability of interaction per unit length of a hyperon Y is given by

$$P_Y = \sum_f \left\{\sigma_{Y+n\to f}(\bar{E})\rho_n + \sigma_{Y+p\to f}(\bar{E})\rho_p\right\} \tag{20}$$

where f accounts for all possible final channels, n and p are neutrons and protons and ρ_n, ρ_p are their local densities. The cross section is evaluated at an invariant energy of the neutrino-nucleon system averaged over the local Fermi sea. We use a threshold energy cut of 30 MeV for quasielastic collisions ($\Lambda \to \Lambda$,$\Sigma \to \Sigma$). Below this energy, we only consider possible $\Sigma \to \Lambda$ processes. Thus, the energy spectra at those low kinetic energies will not be meaningful.

If the hyperon has interacted we select the channel accordingly to their respective probabilities. Finally, once the channel has been selected, we approximately implement Pauli blocking with the following procedure. A random nucleon is selected in the local Fermi sea. Assuming isotropic cross sections in the hyperon-nucleon CM system, we generate a random scattering angle in that system and calculate the hyperon and nucleon momenta. Finally, we boost these momenta to the lab system. If the final nucleon is below the Fermi level (Pauli blocked) we consider that there was no interaction and the hyperon continues its movement.

Otherwise, we have a new hyperon type and/or a new direction and energy.

It should be mentioned that all this procedure does not modify neither the $(\bar{\nu}, lepton)$ cross section, nor the q^2 dependence of that observable, and only the type of outgoing hyperon and its energy and angle distributions are modified. In exclusive reactions, where both the lepton and the hyperon are observed, there could be some changes due to the fact that the lepton distributions would correspond to those of the primary hyperon and not to that of the observed one that could be of a different kind.

IV. RESULTS AND DISCUSSION

The numerical evaluations of the quasielastic production of Σ^0, Σ^- and Λ^0 hyperons induced by antineutrinos from free nucleons have been done using Eq. 4 with the form factors given in table II. The nuclear medium effects due to Fermi motion are incorporated through Eq. 19. The FSI effects, due to hyperon nucleon elastic and charge exchange scattering processes in presence of other nucleons in nuclei are taken into account using a Monte Carlo simulation described in section III C. All the results presented here correspond to muonic antineutrinos.

A. Lepton differential cross sections

We first present the differential cross section for antineutrino induced $\Delta S = 1$ weak quasielastic processes from nucleon and nuclear targets. The sensitivity of the differential cross sections to the axial vector dipole mass has been studied. We have also studied the effect of nuclear medium and final state interactions on the differential cross sections. We find that in the range of energies under analysis, Fermi motion of the nucleons and FSI of the hyperons do not appreciably modify the lepton distributions, except for a scale factor that can also be seen in the total cross sections. As a typical case, we show in Fig. 1 the q^2 dependence on free nucleons and on ^{16}O at $E_{\bar{\nu}} = 1$ GeV. The lowest curve corresponds to the small Σ^+ production which occurs via FSI. The other lines show the results for the Λ, Σ^- and Σ^0. The results without FSI are very close to the free nucleon ones and are not shown. Even the full model curves have the same shape. Thus, we find that nuclear data could still be used to investigate the q^2 dependence of the form factors in the hyperons

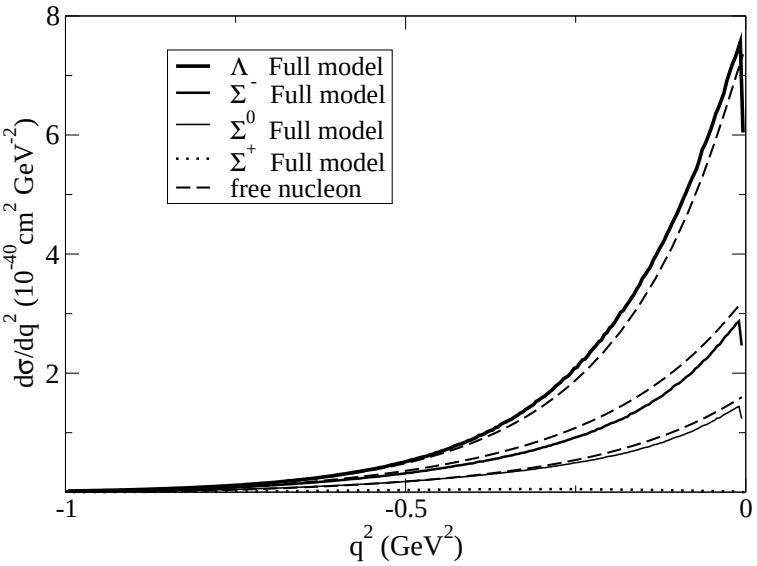

FIG. 1: q^2 distributions for the reaction $\bar{\nu} + A \to \mu^+ + Y + X$ at $E_{\bar{\nu}} = 1$ GeV in nucleons and in ^{16}O. In the nuclear case, the cross sections are divided by 8. Solid lines: Full model; dashed lines: hyperon production on a free nucleon. The upper curves correspond to Λ, next to Σ^-, next to Σ^0. Dotted line: Σ^+.

sector. However, as shown in Fig. 2, the M_A dependence is very mild. This is specially so at low energies and for the case of Σ production. Only at relatively large antineutrino energies and for Λ production the cross section shows some sensitivity to this parameter.

B. Hyperons spectra

We show in Fig. 3 the hyperons spectra with and without FSI for 1 GeV antineutrinos. The main effect of FSI is a redistribution of strength, pushing the spectra towards lower energies. This is due to quasielastic collisions with the nucleons and also to inelastic scattering, in which the kind of hyperon changes and part of the energy is passed to the nucleons. Also remarkable is the appearance of Σ^+ through the $\Sigma^0 + p \to \Sigma^+ + n$ and $\Lambda + p \to \Sigma^+ + n$ processes. This channel is not present on free nucleons and will be further discussed in the next section. We should recall here that our MC code does not include neither the effects of the real part of the optical potentials nor interactions of particles with kinetic energies below 30 MeV. Therefore, the results at those low energies are not meaningful and are shown only

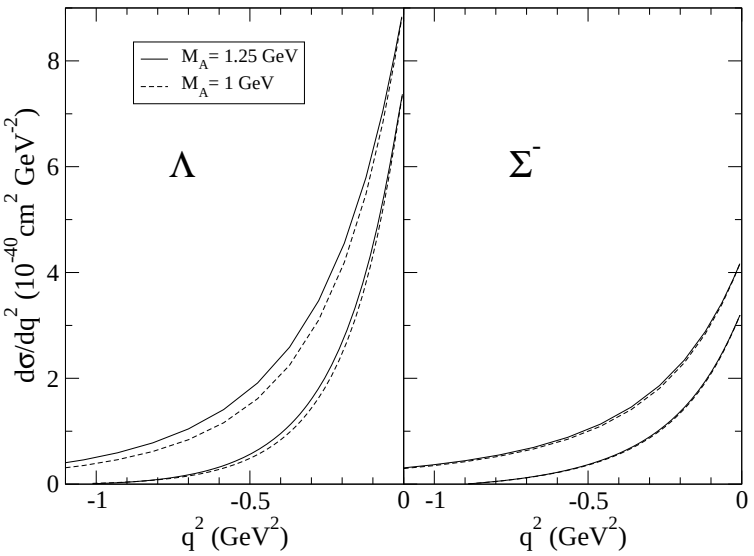

FIG. 2: q^2 distributions for the reaction $\bar{\nu} + N \to \mu^+ + Y + N$ at $E_{\bar{\nu}} = 1$ (lower curves) and 3 GeV (upper curves) for two M_A values.

for illustrative purposes.

C. Total Cross sections

We present in figures 4-6 the numerical results for the muonic antineutrino total cross sections $\sigma(E_{\bar{\nu}})$ for free nucleons and for ^{16}O and ^{56}Fe, divided in the nuclear case by the number of "active" nucleons, with and without the inclusion of FSI. We see from these figures that

(i) The effect of the Fermi motion of the initial nucleons is quite small on the quasielastic production of hyperons even for a heavy nucleus like ^{56}Fe as shown in figures 4-6. Of course, this effect is larger at energies, not shown in the figures, very close to threshold, where the cross sections are very small. Actually, in the nuclear case, the production threshold changes due to Fermi motion although the exact size of the effect depends on the hyperon nucleus optical potential.

(ii) The effect of hyperons FSI leads to an increase of the cross sections for Λ production and a decrease of Σ^0 and Σ^- production cross sections. This change in the cross section per nucleon increases with the charge and mass number of the nucleus and is larger for ^{56}Fe as

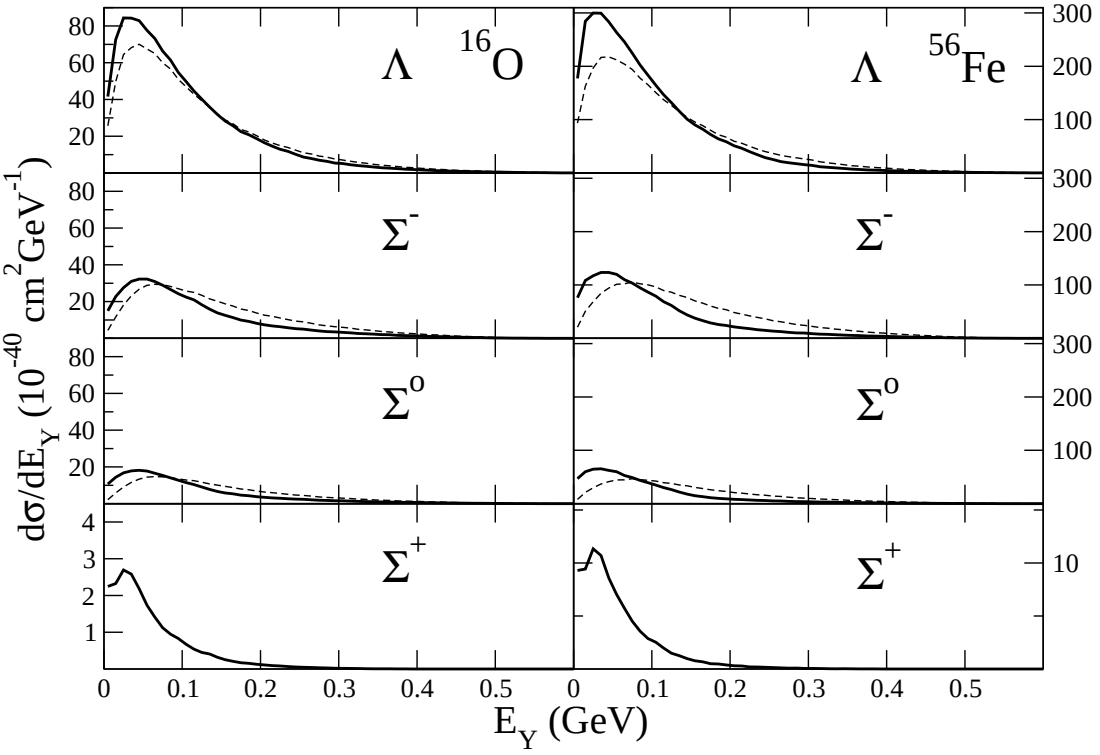

FIG. 3: Hyperons energy distributions as a function of the hyperon kinetic energy for the reaction $\bar{\nu} + A \to \mu^+ + Y + X$ at $E_{\bar{\nu}} = 1$ GeV. Left(right) side corresponds to $^{16}O(^{56}Fe)$. Solid line: full model, dashed line: without final state interaction.

compared to ^{16}O. This is because $\Sigma^{-,0}$ can disappear through the quasielastic processes like $\Sigma^- + p \to \Lambda^0 + n$, $\Sigma^0 + n \to \Lambda^0 + n$ and others, while the inverse process of depletion of Λ is also allowed, but inhibited due to the difference in masses. In addition to these strong processes leading to the depletion of Σ^0, they are further depleted by the electromagnetic decay $\Sigma^0 \to \Lambda + \gamma$. This has not been included in the calculation as the mean life guarantees that the decay will occur out of the nucleus and can be easily taken into account when comparing with data.

(iii) For free nucleon targets, the cross section for production of Λ is always greater than the cross section for production of Σ^0. The ratio $R = \frac{\sigma(\bar{\nu}+p\to\mu^+ + \Sigma^0)}{\sigma(\bar{\nu}+p\to\mu^+ + \Lambda)}$ reaches an asymptotic value of around 0.3 which is consistent with older results of Cabibbo and Chilton [31] but is considerably different with the prediction of a relativistic quark model due to Finjord

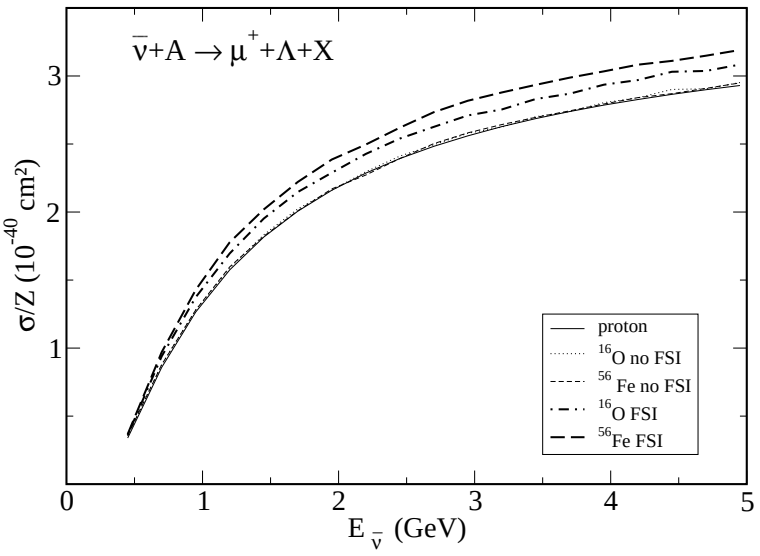

FIG. 4: Cross section for Λ production induced by a muonic antineutrino divided by the number of protons.

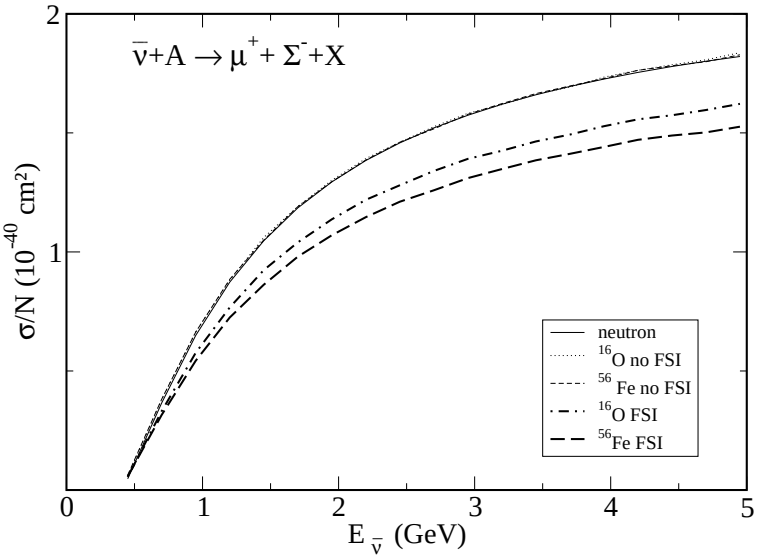

FIG. 5: Cross section for Σ^- production induced by a muonic antineutrino divided by the number of neutrons.

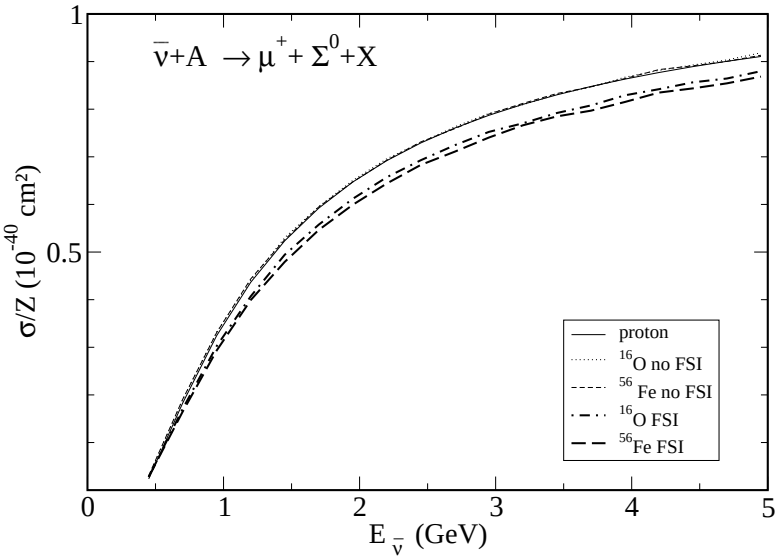

FIG. 6: Cross section for Σ^0 production induced by a muonic antineutrino divided by the number of protons.

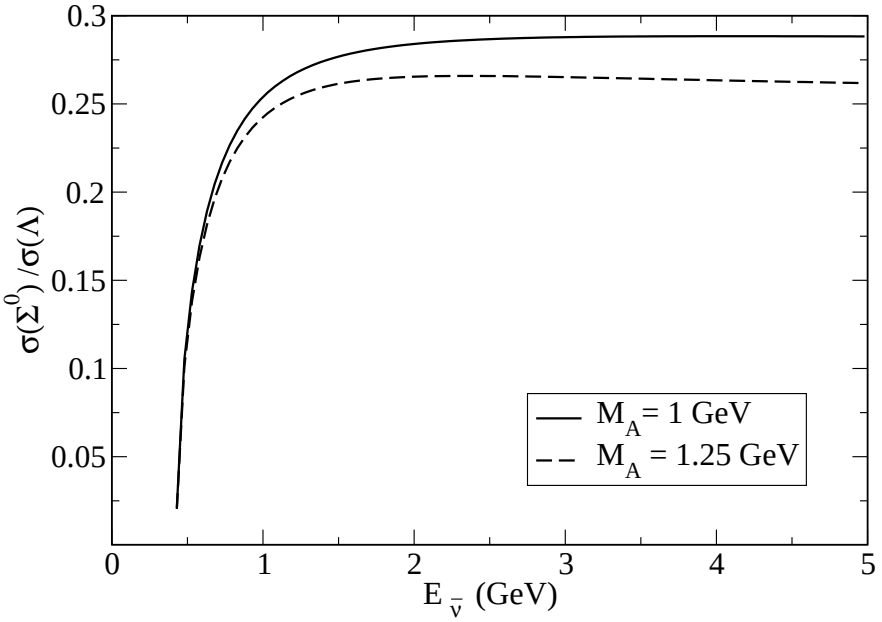

FIG. 7: The ratio $R = \sigma(\bar{\nu} + p \rightarrow \mu^+ + \Sigma^0)/\sigma(\bar{\nu} + p \rightarrow \mu^+ + \Lambda)$ as a function of the antineutrino energy.

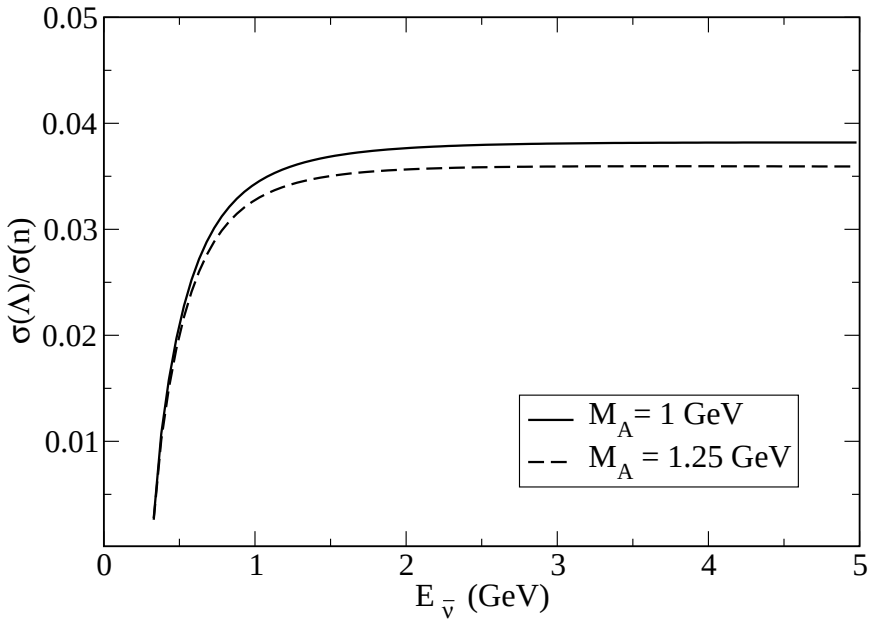

FIG. 8: The ratio $R = \sigma(\bar{\nu} + p \to \mu^+ + \Lambda)/\sigma(\bar{\nu} + p \to \mu^+ + n)$ as a function of the antineutrino energy.

and Ravndal[33]. This ratio is considerably smaller at low energies due to threshold effects which suppress Σ^0 production compared to Λ production. The sensitivity of this ratio for two values of the axial vector dipole mass M_A is shown in Fig. 7.

(iv) For free nucleon targets, using SU(3) symmetric form factors, the ratio of cross sections for $\Delta S = 0$ and $\Delta S = 1$ induced processes by antineutrinos, i.e. $R = \frac{\sigma(\bar{\nu}+p\to\mu^+ + \Lambda)}{\sigma(\bar{\nu}+p\to\mu^+ + n)}$ reaches an asymptotic value of 0.04. This value comes mainly due to the Cabibbo suppression and from the threshold effects which are quite large in this case. The energy dependence of this ratio along with its sensitivity to the value of the axial vector dipole mass M_A is shown in Fig. 8.

(v) In Fig. 9, we show the cross section for Σ^+ production. Whereas in the other channels FSI produces simply a correction to the direct process, in this case all events come from FSI and therefore the cross section is very sensitive to the relatively unknown hyperon nucleon cross sections. This channel is a source of positive pions induced by a charged current antineutrino process, but the cross section is very small and other sources, like charge exchange reactions of pions produced inside the nuclei by other processes, as discussed below,

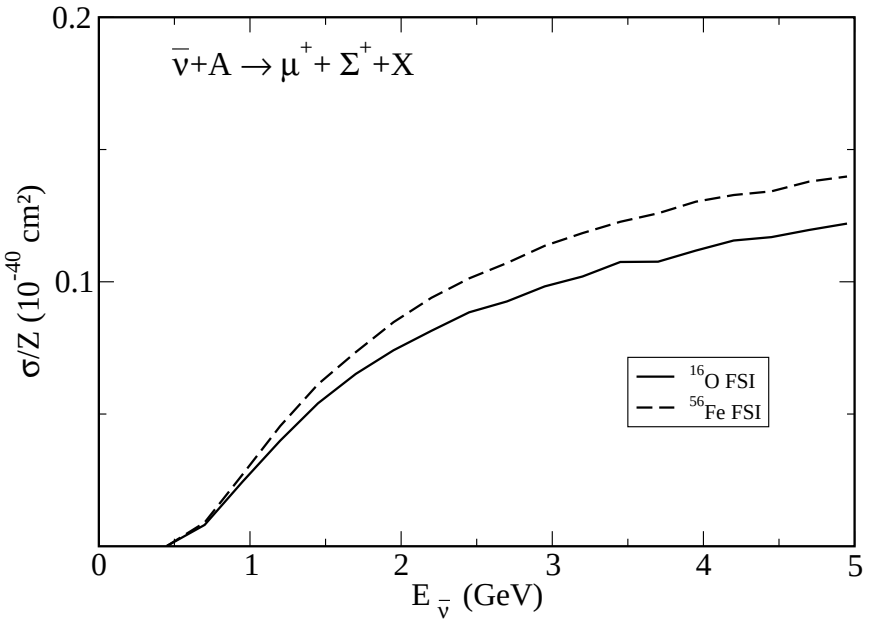

FIG. 9: Cross section for Σ^+ production induced by a muonic antineutrino divided by the number of protons as a function of the antineutrino energy.

will be more important.

D. Pion production from hyperons

Currently, there is considerable interest in the weak pion production cross sections. For these processes, Δ excitation followed by its decay will be dominant at intermediate energies given its strong coupling to the pion nucleon system. However, two aspects deplete its contribution to the pion production in nuclei. First, the mean life of the Δ is very short. Thus, it decays inside the nucleus and part of the pions are absorbed and don't come out of the nucleus. This is quite different to the hyperons case which decay weakly into pions. The hyperons large mean life implies that most of the times they decay already far from the nucleus avoiding the pion absorption. On the other hand, the mass of the Δ implies that the cross section decreases at low enough energies faster than for the Λ and Σ cases. These two factors could partially compensate for the $tan^2\theta_c$ suppression.

We show in Fig. 10 our results for pion production, obtained using the experimental

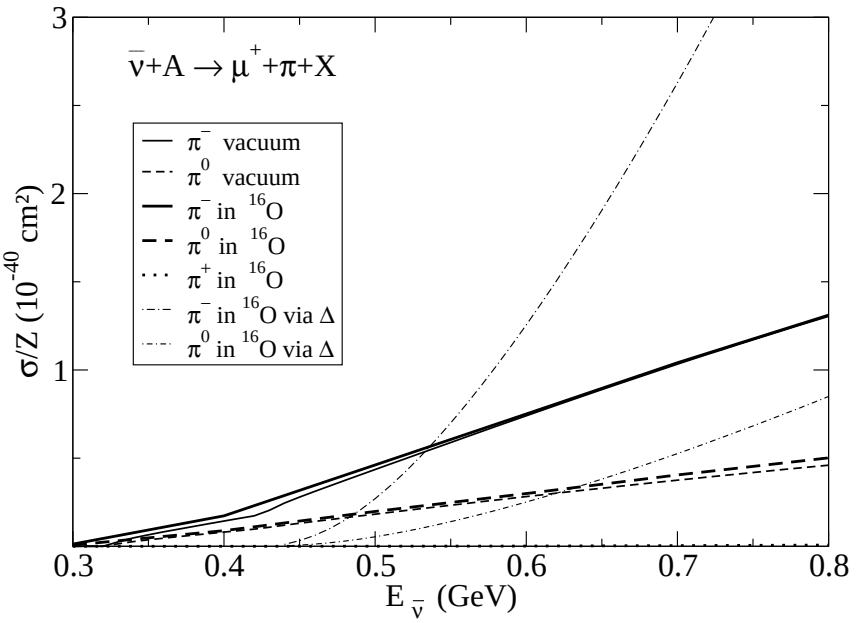

FIG. 10: Cross section for π production via an intermediate hyperon induced by a muonic antineutrino divided by the number of protons as a function of the antineutrino energy. Results compared with pions produced via Δ excitation.

branching ratios for the hyperons and the previous calculations for the hyperon production cross sections. We also show results derived from the Δ production cross section in ^{16}O of ref. [26] which incorporated pion absorption. In that paper, only the total number of pions (or Δ's) was obtained. In order to compare with the current results, we have used the corresponding isospin factors to assign the charges of the pions (relative weights for $p \to \Delta^0 \to p\pi^-$, $p \to \Delta^0 \to n\pi^0$ and $n \to \Delta^- \to n\pi^-$ are 1/9, 2/9 and 1), thus neglecting possible pion charge exchange reactions. We see that at low energies pions from hyperon decays dominate and the Δ mechanism becomes dominant at energies above 550 MeV for negative pions and 650 MeV for neutral pions. The importance of the hyperon mechanisms would be larger for heavier nuclei, where pion absorption would suppress more strongly other competing mechanisms which produce the pions inside the nucleons.

V. SUMMARY AND CONCLUSIONS

We have studied the weak charged current induced quasielastic production of Λ and Σ hyperons from nucleons and nuclei. The transition form factors for the nucleon-hyperon transitions determined from an analysis experimental data on neutrino nucleon scattering and semileptonic decays of hyperons using Cabibbo theory with SU(3) symmetry have been applied to calculate the the total and differential cross sections for lepton and hyperon production from nucleon and nuclear targets. The nuclear medium and final state interaction effects have been calculated for the hyperon production from nuclear targets like ^{16}O and ^{56}Fe which are proposed to be used in future detectors for neutrino oscillations and proton decay search experiments. These are calculated in a local Fermi gas model for the nuclei and a simple energy dependent parametrization for the hyperon nucleon scattering cross sections. The hyperon energy distribution for the quasielastic production of Λ, Σ^+ and Σ^0 hyperons induced by antineutrinos and the effect of final state interactions on their energy distribution has been studied. The energy distribution of Σ^+, which are produced only as a consequence of final state interactions has also been presented. Finally the total cross sections for pion production due to decays of hyperons has been presented and compared with the pion production cross sections from Δ production. The main conclusions that can be drawn from our present study are:

(i) The differential cross sections $\frac{d\sigma}{dq^2}$ are more sensitive to the axial vector dipole mass for the case of Λ production than Σ production. However this sensitivity is not as large as compared to to the sensitivity of $\frac{d\sigma}{dq^2}$ to the axial vector dipole mass for neutrino nucleon scattering in the $\Delta S = 0$ sector.

(ii) The effect of nuclear medium effects on $\frac{d\sigma}{dq^2}$ and total cross section σ on the hyperon production is quite small.

(iii) The effect of final state interaction is to increase the cross sections for Λ production and to decrease the cross section for Σ^- and Σ^0 production. The strength of production cross section shifts towards the lower energy of the produced hyperon as a result of final state interactions. The most interesting aspect of the final state interaction is that it leads to the production of Σ^+ hyperons which is of the order of 10% of the Σ^- production cross sections from oxygen targets around 1 GeV. This proportion increases with mass and charge of the nucleus.

(iv) The hyperon production is dominated by Λ production and the production cross section for Σ^0 is small at lower energies but could approach 30% of Λ production as the energy increases and becomes larger than 1.0 GeV.

(v) At low energies, the nuclear pion production induced by antineutrinos through the production of hyperons and their subsequent decays can become important as compared to the antineutrino pion production through the excitation and subsequent decays of Δ resonance. This, for example, happens for neutrino energies E <550(650) MeV) for the case of antineutrino induced $\pi^-(\pi^0)$ production at intermediate energies from ^{16}O target.

Acknowledgments

This work was partially supported by DGI and FEDER funds, contract BFM2003-00856 and by the EU Integrated Infrastructure Initiative Hadron Physics Project contract RII3-CT-2004-506078. S. K. S acknowledges support from the Academic Exchange Agreement beetwen Aligarh M. U. and Valencia U.

APPENDIX: HYPERON NUCLEON CROSS SECTIONS

We present here the parametrizations used in our MC code for the hyperon nucleon cross sections. In the formulas, cross sections are expressed in mb and energies and momenta in GeV. The data used in the fits have been obtained from [49], although we will also quote below the original references. These parametrizations correspond to the best fits (χ-square) to data with the chosen functional form but the statistical errors of the data are quite large and one should use these numbers as simple estimates. The momenta in the formulas always refer to the hyperons

1. $\Lambda + N \rightarrow \Lambda + N$

   $\sigma = (39.66 - 100.45x + 92.44x^2 - 21.40x^3)/p_{LAB}$

   where $x = Min(2.1, p_{LAB})$. Fitted to data for $\Lambda p \rightarrow \Lambda p$ scattering from refs. [50, 51].

2. $\Lambda + N \rightarrow \Sigma^0 N$

   $\sigma = (31.10 - 30.94x + 8.16x^2)p^{\Sigma}_{CM}/p^{\Lambda}_{CM}$

   where $x = Min(2.1, p_{LAB})$. Fitted to data for $\Lambda p \rightarrow \Sigma^0 p$ scattering from [51].

3. $\Sigma^+ + p \to \Sigma^+ + p$

   $\sigma = 11.77/p_{LAB} + 19.07.$

   Fitted to data for $\Sigma^+ p \to \Sigma^+ p$ scattering from refs. [52].

4. $\Sigma^- + p \to \Sigma^- + p$

   $\sigma = 22.40/p_{LAB} - 1.08.$

   Fitted to data for $\Sigma^- p \to \Sigma^- p$ scattering from [52].

   The rest of the channels have not been fitted and we have used either isospin symmetry, detailed balance or assumed a similar size and energy dependence to the available channels.

5. $\sigma_{\Lambda+n\to\Sigma^- p} = \sigma_{\Lambda+p\to\Sigma^+ n} = 2\sigma_{\Lambda+n\to\Sigma^0+n} = 2\sigma_{\Lambda+p\to\Sigma^0+p}$, $\sigma_{\Sigma^-+n\to\Sigma^-+n} = \sigma_{\Sigma^++p\to\Sigma^++p}$ and $\sigma_{\Sigma^++n\to\Sigma^++n} = \sigma_{\Sigma^-+p\to\Sigma^-+p}$ using isospin symmetry.

   With these, we already have all channels with a Λ in the initial state. The missing channels with a Λ in the final state are obtained by detailed balance, so that

$$p_{ab}^2 \sigma_{ab\to cd} = p_{cd}^2 \sigma_{cd\to ab}$$

   where p_{ab} and p_{cd} are the corresponding CM momenta. The rest of the $\Sigma + N$ processes have been taken with a cross section equal to the $\Sigma^- + p \to \Sigma^- + p$. For the case $\Sigma^- + p \to \Sigma^0 + n$ there are a few data points [53] compatible with this value.

---

[1] Y. Fukuda *et al.* [Super-Kamiokande Collaboration], Phys. Rev. Lett. **81** (1998) 1562.

[2] M. H. Ahn *et al.* [K2K Collaboration], Phys. Rev. Lett. **90** (2003) 041801.

[3] J. Monroe [MiniBooNE Collaboration], arXiv:hep-ex/0406048.

[4] P. Adamson *et al.* [MINOS Collaboration], Phys. Rev. D **73** (2006) 072002; MINOS experiment web page http://www-numi.fnal.gov/

[5] D. Casper, Nucl. Phys. Proc. Suppl. **112** (2002) 161; G. P. Zeller, arXiv:hep-ex/0312061.

[6] H. Gallagher, Nucl. Phys. Proc. Suppl. **112** (2002) 188.

[7] Y.Hayato, Nucl. Phys. Proc. Suppl. **112** (2002) 171.

[8] A. Ferrari, P. R. Sala, A. Fasso and J. Ranft, CERN-2005-010.

[9] R. A. Smith and E. J. Moniz, Nucl. Phys. B **43** (1972) 605 [Erratum-ibid. B **101** (1975) 547].

[10] T. K. Gaisser and J. S. O'Connell, Phys. Rev. D **34** (1986) 822.

[11] T. Kuramoto, M. Fukugita, Y. Kohyama and K. Kubodera, Nucl. Phys. A **512** (1990) 711.

[12] S. K. Singh and E. Oset, Nucl. Phys. A **542** (1992) 587; S. K. Singh and E. Oset, Phys. Rev. C **48** (1993) 1246.

[13] A. K. Mann, Phys. Rev. D **48**, 422 (1993).

[14] Y. Umino and J. M. Udias, Phys. Rev. C **52** (1995) 3399; Y. Umino, J. M. Udias and P. J. Mulders, Phys. Rev. Lett. **74** (1995) 4993.

[15] H. C. Kim, J. Piekarewicz and C. J. Horowitz, Phys. Rev. C **51** (1995) 2739.

[16] G. Co', C. Bleve, I. De Mitri and D. Martello, Nucl. Phys. Proc. Suppl. **112**, 210 (2002).

[17] H. Nakamura and R. Seki, Nucl. Phys. Proc. Suppl. **112** (2002) 197.

[18] O. Benhar, N. Farina, H. Nakamura, M. Sakuda and R. Seki, Phys. Rev. D **72** (2005) 053005.

[19] A. Meucci, C. Giusti and F. D. Pacati, Nucl. Phys. A **744** (2004) 307.

[20] J. Nieves, J. E. Amaro and M. Valverde, Phys. Rev. C **70** (2004) 055503 [Erratum-ibid. C **72** (2005) 019902].

[21] J. Nieves, M. Valverde and M. J. Vicente Vacas, Phys. Rev. C **73** (2006) 025504.

[22] M. C. Martinez, P. Lava, N. Jachowicz, J. Ryckebusch, K. Vantournhout and J. M. Udias, Phys. Rev. C **73** (2006) 024607.

[23] E. A. Paschos, L. Pasquali and J. Y. Yu, Nucl. Phys. B **588** (2000) 263; E. A. Paschos and J. Y. Yu, Phys. Rev. D **65** (2002) 033002; O. Lalakulich and E. A. Paschos, Phys. Rev. D **71** (2005) 074003.

[24] T. Sato, D. Uno and T. S. H. Lee, Phys. Rev. C **67** (2003) 065201.

[25] H. C. Kim, S. Schramm and C. J. Horowitz, Phys. Rev. C **53** (1996) 2468; ibidem, **53** (1996) 3131.

[26] S. K. Singh, M. J. Vicente Vacas and E. Oset, Phys. Lett. B **416** (1998) 23 [Erratum-ibid. B **423** (1998) 428]; M. S. Athar, S. Ahmad and S. K. Singh, Eur. Phys. J. A **24** (2005) 459.

[27] J. Marteau, J. Delorme and M. Ericson, Nucl. Instrum. Meth. A **451** (2000) 76.

[28] E. A. Paschos, J. Y. Yu and M. Sakuda, Phys. Rev. D **69** (2004) 014013.

[29] T. Leitner, L. Alvarez-Ruso and U. Mosel, arXiv:nucl-th/0601103; L. Alvarez-Ruso, T. Leitner

and U. Mosel, arXiv:nucl-th/0601021; T. Leitner, L. Alvarez-Ruso and U. Mosel, Prog. Part. Nucl. Phys. **57**, 395 (2006).

[30] W. Cassing, M. Kant, K. Langanke and P. Vogel, arXiv:nucl-th/0601090.

[31] N. Cabibbo, Phys. Rev. Lett. **10** (1963) 531; N. Cabibbo and F. Chilton, Phys. Rev. **137** (1965) B1628.

[32] A.Pais, Annals Phys. **63** (1971) 361; C. H. Llewellyn Smith, Phys. Rept. **3** (1972) 261; R. E. Shrock, Phys. Rev. D **12** (1975) 2049; A. A. Amer, Phys. Rev. D **18** (1978) 2290; H. K. Dewan, Phys. Rev. D **24**, 2369 (1981); S. L. Mintz, Int. J. Mod. Phys. A **20** (2005) 1212.

[33] J. Finjord and F. Ravndal, Nucl. Phys. B **106** (1976) 228.

[34] T. Eichten *et al.*, Phys. Lett. B **40** (1972) 593.

[35] O. Erriquez *et al.*, Nucl. Phys. B **140** (1978) 123.

[36] J. Brunner *et al.* [SKAT Collaboration], Z. Phys. C **45** (1990) 551.

[37] There are some experiments where production of strange mesons has also been studied for example N. J. Baker *et al.*, Phys. Rev. D **24** (1981) 2779; H. Deden *et al.*, Phys. Lett. B **58**, 361 (1975); W. A. Mann, T. Kafka, M. Derrick, B. Musgrave, R. Ammar, D. Day and J. Gress, Phys. Rev. D **34** (1986) 2545.

[38] K. S. McFarland, Eur. Phys. J. A **24S2**, 187 (2005); D. Drakoulakos *et al.* [Minerva Collaboration], arXiv:hep-ex/0405002.

[39] J. D. Bjorken and S. D. Drell, Relativistic Quantum Fields (McGraw-Hill, New York, 1965)

[40] J. M. Gaillard and G. Sauvage, Ann. Rev. Nucl. Part. Sci. **34** (1984) 351.

[41] N. Cabibbo, E. C. Swallow and R. Winston, Ann. Rev. Nucl. Part. Sci. **53** (2003) 39 [arXiv:hep-ph/0307298].

[42] J.F. Donoghue, B.R. Holstein and S.W. Klimt, Phys. Rev. D **35** (1987) 934; F. Schlumpf, Phys. Rev. D**51** (1995) 2262; J. Anderson and M. Luty, Phys. Rev. D **47** (1993) 4975; R. Flores-Mendieta, E. Jenkins and A.V. Manohar, Phys. Rev. **D** 58(1998)094028.

[43] S. Galster, H. Klein, J. Moritz, K. H. Schmidt, D. Wegener and J. Bleckwenn, Nucl. Phys. B **32** (1971) 221.

[44] W. M. Alberico, S. M. Bilenky and C. Maieron, Phys. Rept. **358** (2002) 227 [arXiv:hep-ph/0102269].

[45] L. A. Ahrens *et al.*, Phys. Rev. D **35** (1987) 785.

[46] R.Gran et al.; K2K Collaboration, hep-ex/0603034.

[47] C. W. De Jager, H. De Vries and C. De Vries, Atom. Data Nucl. Data Tabl. **36** (1987) 495.

[48] E. Oset, P. Fernandez de Cordoba, L. L. Salcedo and R. Brockmann, Phys. Rept. **188** (1990) 79.

[49] http://nn-online.org/

[50] G. Alexander, U. Karshon, A. Shapira, G. Yekutieli, R. Engelmann, H. Filthuth and W. Lughofer, Phys. Rev. **173** (1968) 1452; B. Sechi-Zorn, B. Kehoe, J. Twitty and R. A. Burnstein, Phys. Rev. **175** (1968) 1735.

[51] J. A. Kadyk, G. Alexander, J. H. Chan, P. Gaposchkin and G. H. Trilling, Nucl. Phys. B **27** (1971) 13; J. M. Hauptman, J. A. Kadyk and G. H. Trilling, Nucl. Phys. B **125** (1977) 29.

[52] H. G. Dosch, R. Engelmann, H. Filthuth, V. Hepp and E. Kluge, Phys. Lett. **21** (1966) 236; H.A. Rubin and R.A. Burnstein, Phys. Rev. **159** (1967) 1149; F. Eisele, H. Filthuth, W. Foehlisch, V. Hepp and G. Zech, Phys. Lett. B **37** (1971) 204; G. R. Charlton *et al.*, Phys. Lett. B **32** (1970) 720 .

[53] R. Engelmann et al., Phys. Lett. **21** (1966) 587.